JOURNAL OF MATERIALS SCIENCE 23 (1988) 150–160

Eutectoid decomposition mechanisms in hypoeutectoid Ti–X alloys

H. J. LEE*, H. I. AARONSON
Department of Metallurgical Engineering and Materials Science, Carnegie–Mellon University, Pittsburgh, Pennsylvania 15213, USA

A TEM study has been made of the bainite reaction in five hypoeutectoid Ti–X alloys, where X was successively cobalt, chromium, copper, iron and nickel. Rational orientation relationships were demonstrated amongst eutectoid α, eutectoid intermetallic compound and the β matrix in Ti–Ni, Ti–Co and Ti–Cr. Formation of Ti_2Co at $\alpha:\beta$ boundaries was observed. Eutectoid α in bainite was found to be slightly misoriented with respect to proeutectoid α, indicating that it is separately nucleated, perhaps sympathetically, rather than the result of the continued growth of proeutectoid α. Eutectoid Ti_2Co and Ti_2Cu crystals in bainite were approximately equiaxed whereas $Ti–Cr_2$ crystals were elongated, a result ascribed to a ledge height-to-spacing ratio h/λ at intermetallic compound crystal : β boundaries approaching that of eutectoid $\alpha:\beta$ boundaries in Ti–Cr but not in the other two systems. In the Ti–Fe alloy, eutectoid α and eutectoid TiFe were directly observed to have ledged interphase boundaries with their β matrix, but with different inter-ledge spacings and growth directions. Observation of pearlite lamellae growing normal to the broad faces of proeutectoid α plates in the Ti–Ni alloy indicates that this mode of eutectoid decomposition, like that of bainite, can develop from partially coherent interphase boundaries. The suggestion was offered that pearlite forms when λ approaches h at the nucleating proeutectoid $\alpha:\beta$ interface and that bainite develops when $\lambda \ggg h$ at this interface.

1. Introduction

Franti *et al.* [1] have surveyed eutectoid decomposition processes in ten Ti–X systems, where X was successively bismuth, cobalt, chromium, copper, iron, manganese, nickel, lead, palladium and platinum. One of their most important findings was that the bainite reaction is the primary, and usually the only, mechanism through which the eutectoid reaction occurs in pronouncedly hypoeutectoid alloys in all of these systems but Ti–Cu. To avoid unnecessary entanglement in definitional problems [2], we immediately note that the term "bainite" is used here to describe the non-lamellar [2], non-cooperative [3], competitive [4] mode of eutectoid decomposition. On this definition, precipitation of the second low-temperature phase during generation of the eutectoid microstructure is essential. As Franti *et al.* [1] used only optical microscopy during their investigation, some important questions raised during this and a previous study of the same type specifically directed at Ti–Cr alloys [5, 6] have remained unanswered. In the present work, transmission electron microscopy was the principal investigative tool employed and has been utilized to examine some of these problems in alloys selected from among those studied by Franti *et al.* The results of the present investigation will be discussed primarily upon the basis of a recent theoretical treatment of fundamental differences between the bainitic and pearlitic modes of eutectoid decomposition [7]. Some contributions will also be offered, however, to knowledge of the proeutectoid α reaction (as a supplement to recent detailed TEM studies of this transformation [8–10]), and also of the pearlite reaction, the lamellar, cooperative [3] counterpart to the bainitic mode of eutectoid decomposition.

2. Experimental procedures

The alloys were prepared at the Rockwell International Science Center. A 0.030 kg button of each was melted 12 times. All were then homogenized for 7 days at 1000° C *in vacuo*. Table I lists the alloy compositions used. Table II summarizes the eutectoid temperature and composition, and also the structure of the intermetallic compound in each Ti–X system investigated. In all of them, the β matrix is bcc and is retained during quenching to room temperature (except for some fine-scale omega-phase precipitation).

Specimens 0.01 m × 0.005 m × 0.001 m were cut from each of these homogenized alloys for heat treatment. These specimens were cleaned sequentially in benzene, acetone and methanol and then wrapped in tantalum foil. Each specimen was individually encapsulated in Vycor. The capsules were evacuated and flushed repeatedly with purified helium and lightly torched after each flush to drive off adsorbed gases; the capsules were finally sealed off under a dynamic vacuum of better than 5×10^{-6} torr.

The encapsulated specimens were solution annealed

Present address: Technical Research Laboratory, Pohang Iron and Steel Co. Ltd, P.O. Box 36, Pohang 680, Korea.

0022–2461/88 $03.00 + .12

TABLE I Alloy compositions

Alloy	X (wt %)	X (at %)	O (wt %)	N (wt %)
Ti–Co	3.9	3.2	–	–
Ti–Cr	7.2	6.6	0.034	0.003
Ti–Cu	6.0	4.6	–	–
Ti–Fe	5.2	4.5	–	–
Ti–Ni	4.0	3.3	–	–

at 1273 K (in the β-phase field) for 1200 sec, isothermally reacted in stirred, graphite protected and deoxidized lead pots and quenched by shattering the capsules under iced brine.

TEM specimens were initially prepared by electropolishing. Because this process is now known to introduce large quantities of hydrogen into titanium alloys, resulting in formation of the "interface phase" [11], its use was discontinued. TEM specimens were subsequently produced with a Gatan ion miller, using a gun voltage of 6 kV and a gun current of 0.3 to 0.5 mA. Jeol 100C and Jeol 120CX microscopes were used for the TEM studies.

3. Experimental results

3.1. Proeutectoid alpha reaction

Menon and Aaronson have reported detailed studies of sympathetic nucleation [8] and of interphase boundary structure [10] in proeutectoid α microstructures formed in a Ti–7.15 wt % Cr (6.6 at % Cr) alloy. The observations in this section, made on a Ti–3.9 wt % Co (3.2 at % Co) alloy, helped to demonstrate the generality of these findings, and in the case of growth ledge structures, to extend them to more complex morphological situations.

That edge-to-edge sympathetic nucleation plays an important role in the lengthening of proeutectoid α plates has long been known from optical microscopy studies [5]. Menon and Aaronson [8] have confirmed this observation by means of TEM and have shown that adjacent components of the α plates are misoriented by angles of up to 1 to 2°. Fig. 1 demonstrates that a similar situation obtains during proeutectoid α plate formation in the Ti–Co alloy. Arrowheads point out five small-angle $\alpha:\alpha$ boundaries within one of the plates of this figure. Small, but perceptible, changes in contrast from one component of this plate to the next along the length of the plate indicate that they are slightly misoriented with respect to each other. Indications of dislocation contrast at some of these boundaries support the deduction that they are of the small-angle type.

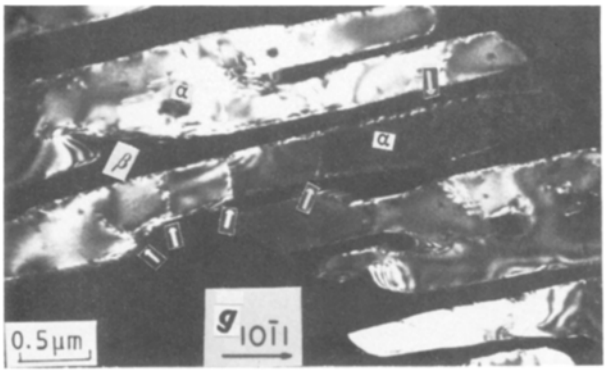

Figure 1 Dark-field micrograph of typical intragranular Widmanstatten proeutectoid α plates in Ti–3.9 wt % Co reacted for 600 sec at 903 K. Arrows indicate small-angle boundaries formed by sympathetic nucleation.

The other observations on proeutectoid α to be presented deal primarily with growth ledges. Because the strain fields of adjacent ledges do not cancel at some distance from the ledges, the contrast associated with ledges tends to be both broader and more pronounced than that of misfit dislocations [12]. The ability of ledges to displace thickness fringes is also useful in distinguishing them from misfit dislocations [13]. Fig. 2 shows growth ledges at the sides and leading edge of an α lath, and also misfit dislocations, particularly at the edge. Note the broad, dark lines produced by the ledges (marked L) and the narrow, rather faint lines corresponding to the misfit dislocations (marked D). At the lath leading edge, the misfit dislocations make an angle greater than 60°

TABLE II Eutectoid region of Ti–X systems studied [1, 32]

Alloy system	Eutectoid composition wt % (at %)	Eutectoid temperature (K)	Intermetallic compound
Ti–Co	9.5(8.0)	958	Ti_2Co fcc with 96 atoms/unit cell a_0 = 1.1306 nm
Ti–Cr	15.0(14.0)	940	$TiCr_2$ fcc (C15) a_0 = 0.6943 nm
Ti–Cu	7.1(5.5)	1071	Ti_2Cu tetragonal ($MoSi_2$-type) a_0 = 0.297, c_0 = 1.090 nm
Ti–Fe	14.5(13.0)	858	TiFe (CsCl type) a_0 = 0.2896 nm
Ti–Ni	8.4(6.9)	1043	Ti_2Ni fcc with 96 atoms/unit cell a_0 = 1.1333 nm

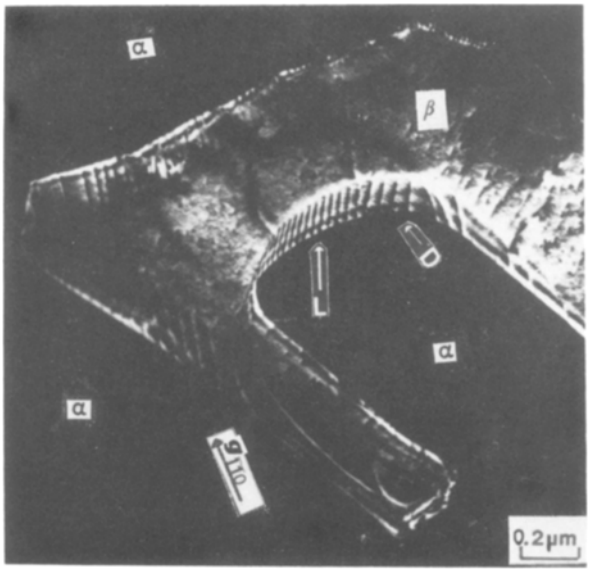

Figure 2 Dark-field micrograph of interfacial structure at the leading and side edges of an α lath in a Ti–5.2 wt % Fe alloy reacted at 823 K for 1.33×10^7 sec. Growth ledges are indicated by L and the misfit dislocations by D. Taken from $(1\,1\,0)_\beta$ reflection.

with respect to the ledges. The growth ledges at the lath leading edge are seen to be closely and quite uniformly spaced. As the right-hand side of the edge is approached, however, the inter-ledge spacing begins to increase, though in a regular fashion. At the side edges of the lath, on the other hand, the ledges are much more widely and irregularly spaced. These observations correspond well with the long-familiar constant lengthening rate of precipitate plates and other anisotropic morphologies [14, 15], to the deduction that, despite their relatively high lengthening rates, plate and lath edges also have a partially coherent structure and must thus grow by means of a ledge mechanism [15–18], and to the expectation that the interfaces orthogonal to those dimensions of a precipitate crystal which are perceptibly smaller than that of the longest, should have a correspondingly wider spacing between their ledges [14, 19]. Although there are many observations of ledge structures on the broad faces of precipitate plates [14, 20], there are only a few on the edges of either plates or laths [21–23]. However, the irregularity of the inter-ledge spacing at the sidewise edges of the lath in Fig. 2 (note that these are also observable at the left-hand edge of this lath via "indentations" in the upper and lower rims of this edge) is similar to that long familiar on plate broad faces [16, 20].

Fig. 3 shows the corresponding edges of a more irregularly shaped α plate or lath. Overall, the curvature of the $\alpha:\beta$ boundary in this region is rather smooth. However, dark-field observations on the growth ledge structure show that there are a number of differently oriented systems of growth ledges simultaneously operative, each of which makes a contribution to the growth process. Nearly all of the four systems of ledges indicated by arrows exhibit some curvature. System 2, in particular, turns through an angle of about 30°. However, the flexibility in orientation of a given system appears to be limited, by a crystallographic effect, by interference from other systems of growth ledges lengthening in a different direction, or possibly by both factors. The much thinner and dimmer lines of misfit dislocations are visible within System 4, where they make a large angle with respect to the growth ledges.

Fig. 4 is a weak-beam, dark-field micrograph of an intricately shaped $\alpha:\beta$ interface whose structure of

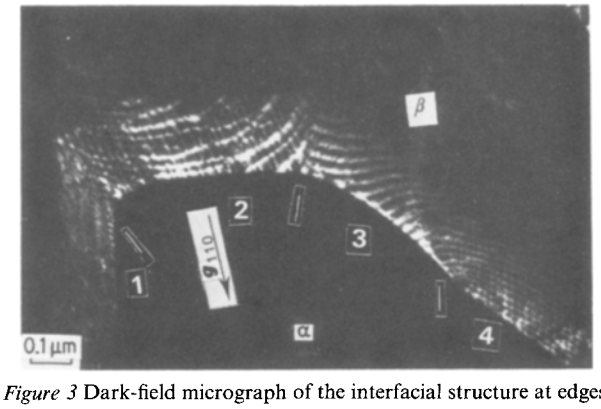

Figure 3 Dark-field micrograph of the interfacial structure at edges of a more irregularly shaped α plate in a Ti–3.9 wt % Co alloy reacted at 903 K for 600 sec, showing a number of differently oriented systems of growth ledges.

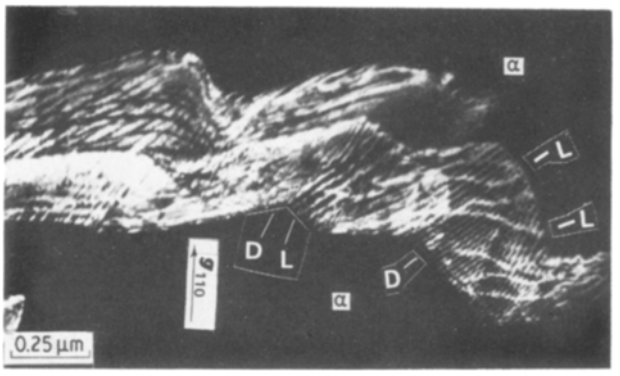

Figure 4 Dark-field micrograph of the interfacial structure of an intricately shaped α plate in Ti–3.9 wt % Co alloy reacted at 898 K for 2400 sec. The growth ledges marked L are irregularly spaced, while the misfit dislocations marked D are more closely and regularly spaced.

ledges and misfit dislocations appears to be even more complex. Because of the weak-beam technique [24], the misfit dislocations are much better displayed in this micrograph. Several sets of them and of growth ledges are pointed out by lines added to this micrograph.

These observations further document the ubiquity of partial coherency and also demonstrate that interphase boundary structures, because of their complexity and irregularity, must continue to be studied experimentally as well as theoretically in order that their structural, energetic and kinetic properties may be properly appreciated.

3.2. Bainite reaction

Figs 5a and b are bright- and dark-field micrographs of the same area in the Ti–Co alloy, showing a single incomplete row of isolated Ti_2Co precipitates at three junctions between adjacent, parallel α plates. Fig. 5b demonstrates that the Ti_2Co crystals in a given row exhibit a pronounced, but perhaps not a complete, tendency to have the same crystallographic variant of their orientation relationships. Note that the right-hand row in Fig. 5a is not visible in Fig. 5b; the morphology of the precipitates in this row is also appreciably different from that of the precipitates in the middle row, though somewhat similar to those in the left-hand row. Evidently the precipitates in the right-hand row were oriented parallel to a different crystallographic variant. Because these precipitates could have nucleated at either of the two pairs of $\alpha:\beta$ boundaries which existed prior to consolidation into two single $\alpha:\alpha$ boundaries, and substantial irregularities in the path of these boundaries are usual, such utilization of multiple variants is to be expected. The angle between the principal facet plane and that of a grain boundary has been shown to affect, often significantly, the activation free energy for critical nucleus formation at the grain boundary [25, 26]. Equivalent considerations should apply during nucleation at an interphase boundary. Similarly, precipitates which employ the same variants of their orientation relationships with respect to α and β are to be expected when the broad faces of α plates are substantially planar, as was evidently the case for the sideplates which formed the left-hand and central rows in Figs 5a

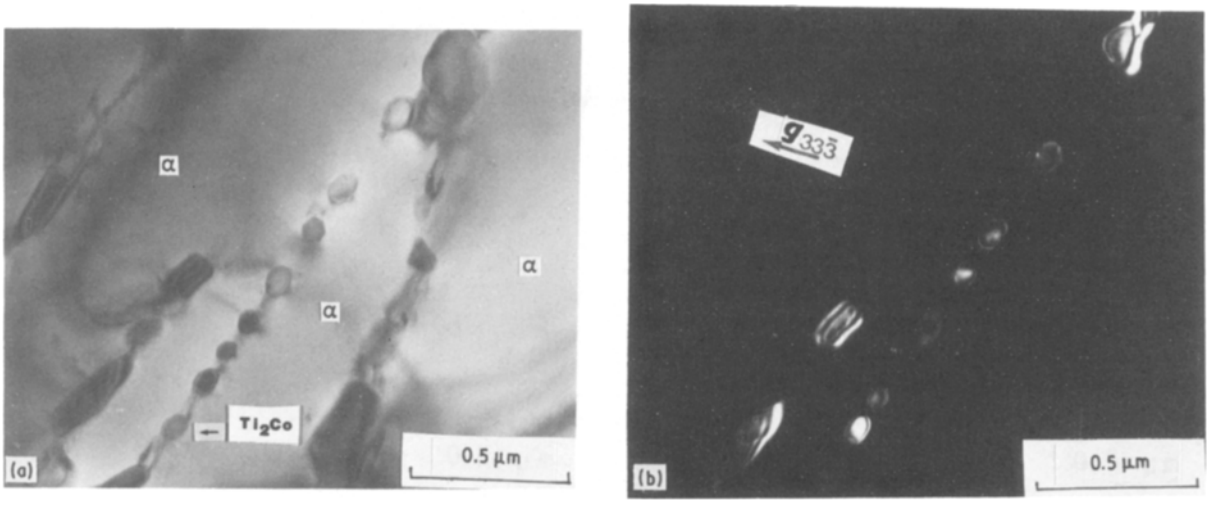

Figure 5 Transmission electron micrographs of fully reacted bainite microstructure in Ti–3.9 wt % Co alloy reacted at 898 K for 7200 sec; (a) bright-field micrograph showing rows of Ti_2Co crystals between proeutectoid α plates; (b) dark-field micrograph in which the right-hand row of compound crystals is invisible.

and b. This effect is now well established in Fe–C–X alloys during the so-called "interphase precipitation" of alloy carbides [27, 28]. Fig. 6 shows that the overall morphology of the intermetallic compound Ti_2Cu, formed during the bainite reaction in Ti–6.0 wt % Cu, is similar to that in Ti–3.9 wt % Co.

During the initial optical microscopy study of the bainite reaction in Ti–Cr alloys [5], the question was raised as to whether eutectoid α has the same orientation as the contiguous proeutectoid α or a different one. Eutectoid α is easily identified in hypoeutectoid Ti–Cr alloys as α phase precipitated after $TiCr_2$ has formed at $\alpha:\beta$ boundaries. Particularly at higher reaction temperatures, metastable equilibrium of $\alpha + \beta$ is reached well before the onset of $TiCr_2$ precipitation [29]. In Ti–X systems such as Ti–Co, in which eutectoid decomposition is more rapid, the distinction between the two types of α, though still useful, is obviously not so precise because eutectoid α may develop while proeutectoid α is still growing. This orientation question could not be answered with optical microscopy. Fig. 7 shows a transmission electron micrograph in which faint, but definite low-angle $\alpha:\alpha$ boundaries are seen connecting two rows of Ti_2Co crystals; untransformed β remains between the eutectoid α "layers" which have enveloped the compound particles. These $\alpha:\alpha$ boundaries should mark the location of the $\alpha:\beta$ boundaries prior to Ti_2Co precipitation. Thus eutectoid α can be slightly misoriented with respect to proeutectoid α. This finding suggests that eutectoid α is sympathetically nucleated at the interphase boundaries of proeutectoid α [8], though nucleation of eutectoid α at $\beta:Ti_2Co$ boundaries cannot presently be eliminated from consideration. Continued growth of proeutectoid α, now serving as eutectoid α, without further nucleation, in the manner of the Hultgren [30] mechanism of the bainite reaction, also remains possible but can no longer be considered general. Fig. 7b is a selected-area diffraction pattern encompassing both proeutectoid α and eutectoid α taken from the same area as Fig. 7a. The slight splitting of the α spots in the SAD pattern provides further support for the view that eutectoid α is separately nucleated.

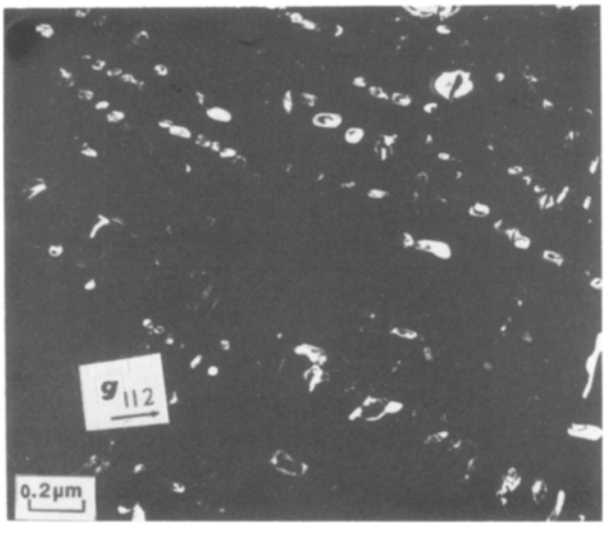

Figure 6 Dark-field micrograph of nearly equiaxed Ti_2Cu crystals in bainite formed in Ti–6.0 wt % Cu alloy reacted at 998 K for 60 sec.

Fig. 8a shows growth ledges on TiFe and on (presumably) eutectoid α in the Ti–5.2 wt % Fe alloy. The spacing between growth ledges and the growth direction of the ledges are seen to be different at the two interphase boundaries. Fig. 8b is a dark-field micrograph displaying with greater clarity the growth ledges on the same TiFe crystal. Equivalent observations have also been made on eutectoid α and $TiCr_2$ in a hypereutectoid Ti–25% Cr alloy [31]; such observations provide an important part of the experimental base for a current theoretical treatment of the differences between the pearlite and bainite reactions [4].

Figs 9a and b are bright- and dark-field micrographs of the bainite structure in a fully transformed specimen of the Ti–7.15 wt % Cr alloy. Unlike bainite in hypoeutectoid Ti–Co (Fig. 5) and Ti–Cu (Fig. 6), the intermetallic compound crystals in Ti–Cr are often pronouncedly elongated, usually in the local growth direction of the bainite structure. The faceting of individual $TiCr_2$ crystals and their usual lack of connection with neighbouring crystals of the same phase are evident. Fig. 9b indicates that the eutectoid α region is composed of smaller, slightly misoriented crystals, e.g. those marked 1 and 2 in this figure. Fig. 9c is a higher magnification view of the same

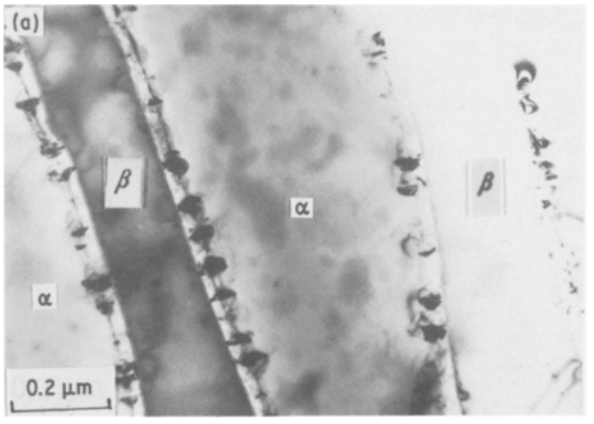

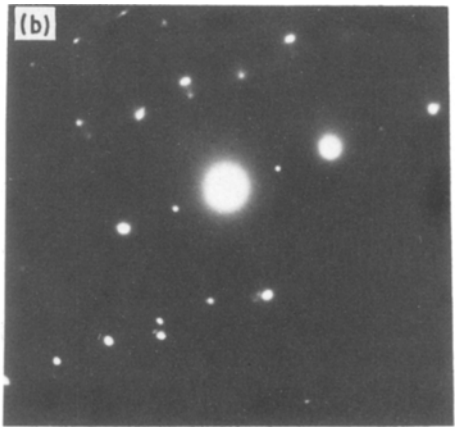

Figure 7 (a) Bright-field micrograph of bainite structure in Ti–3.9 wt % Co reacted at 898 K for 2400 sec showing small-angle boundaries between proeutectoid and eutectoid α. (b) SAD pattern and indexed pattern taken from the same area as Fig. 6. The α phase reflections are split due to the small misorientation between eutectoid and proeutectoid α.

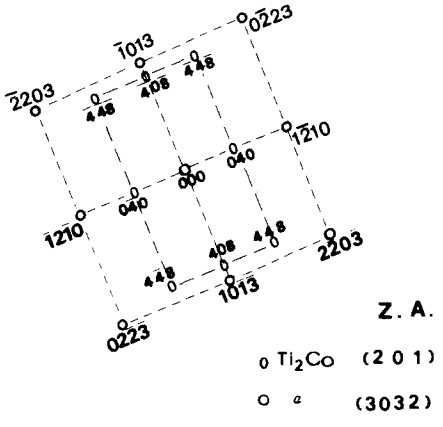

specimen, in which the dislocation structure of small-angle boundaries between adjacent eutectoid α crystals is more clearly displayed. These observations provide evidence for the role played by sympathetic nucleation in the formation of eutectoid α. Twinning of $TiCr_2$, which is evident in Figs 9a and c, is due to ion milling rather than to processes operative during the phase transformation, because it does not occur in electro-polished specimens.

Figs 10a and b are representative SAD patterns and interpretations thereof for determinations of orientation relationships among α (usually of the eutectoid variety), β and intermetallic compound. Table III summarizes all the data of this type obtained during the present investigation. Note that the Burgers orientation relationship invariably obtains between α and β. Both Ti_2Ni and Ti_2Co have the same spatial orientation as their β matrix grain; as shown in Table II, these compounds have the same crystal structure. The same pair of planes is parallel in the β and $TiCr_2$ lattices, but a different pair of directions in these planes is parallel than in the other two systems. Again as indicated in Table II, $TiCr_2$ has a diferent crystal structure – the fcc-type C15 – whereas Ti_2Ni and Ti_2Co have the complex fcc $E9_3$ structure [32]. An equivalent situation is seen to obtain with respect to α and the intermetallic compounds.

3.3. Pearlite reaction

Optical microscopy revealed pearlite in the hypoeutectoid range only in Ti–Cu amongst the ten Ti–X eutectoid systems investigated [1]. During the present study, pearlite was also observed, by means of TEM, in a Ti–4.0 wt % Ni alloy, as illustrated in Fig. 11. The width of these pearlite colonies is clearly too small to have been resolved with optical microscopy. Arrow 1 points to a pearlite colony whose lamellae are perpendicular to the broad faces of the proeutectoid α plates against which they formed, whereas arrow 2 indicates colonies whose lamellae are parallel to the plate broad faces. One might well argue that the latter two colonies evolved from grain-boundary α

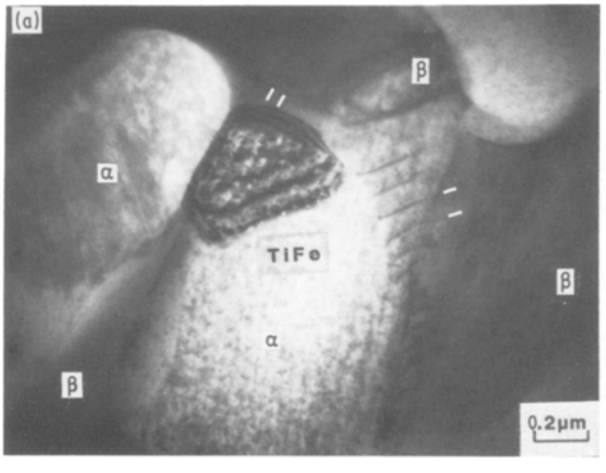

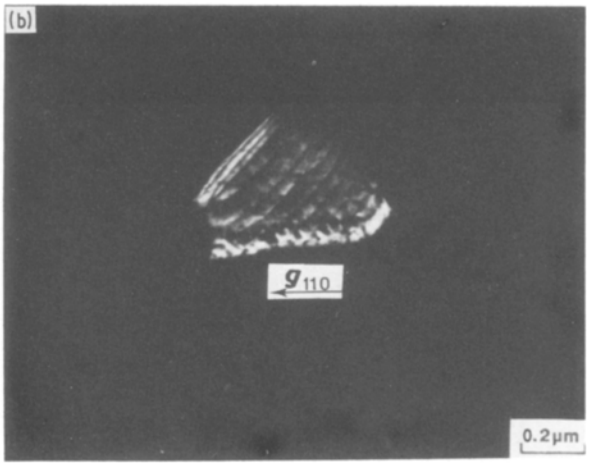

Figure 8 (a) Bright-field micrograph showing different ledge spacings and growth directions on α and TiFe in Ti–5.2 wt % Fe reacted at 823 K for 1.33×10^7 sec. (b) Dark-field micrograph of same area, showing growth ledges in TiFe crystal.

TABLE III Orientation relationship between α, β and intermetallic compound during bainite reaction

Alloy system	β	α	Intermetallic compound
Ti–4.0 wt % Ni	$(0\,1\,1)_\beta \parallel (0\,0\,0\,1)_\alpha \parallel (0\,1\,1)_{Ti_2Ni}$		
	$[1\,1\,1]_\beta \parallel [1\,\bar{2}\,1\,0]_\alpha \parallel [1\,1\,\bar{1}]_{Ti_2Ni}$		
Ti–3.9 wt % Co	$(0\,1\,1)_\beta \parallel (0\,0\,0\,1)_\alpha \parallel (0\,1\,1)_{Ti_2Co}$		
	$[1\,1\,\bar{1}]_\beta \parallel [1\,1\,\bar{2}\,0]_\alpha \parallel [1\,1\,\bar{1}]_{Ti_2Co}$		
Ti–7.15 wt % Cr	$(0\,1\,1)_\beta \parallel (0\,0\,0\,1)_\alpha \parallel (0\,1\,1)_{TiCr_2}$		
	$[1\,1\,\bar{1}]_\beta \parallel [1\,1\,\bar{2}\,0]_\alpha \parallel [2\,1\,\bar{1}]_{TiCr_2}$		

allotriomorphs located outside the electron-transarent area of the thin foil [33]. However, the Ti_2Ni lamellae of the colony at arrowhead 1 almost certainly nucleated at the partially coherent broad faces of the proeutectoid α plates, if not within the thin foil then not too far above or below its limits. Taken in conjunction with the recent observation that the broad faces of grain-boundary α allotriomorphs in the Ti–7.15 wt % Cr alloy are densely ledged [34], and thus must be partially coherent, this observation indicates that the view that such boundaries do not favour pearlite formation [3] must be reconsidered.

Fig. 12 provides an interesting illustration of the simultaneous growth of pearlite from both broad faces of adjacent, parallel proeutectoid α plates. Even though the two broad faces were only about 0.5 μm apart, and the compound lamellae, here Ti_2Cu, were thus able to lengthen only about half as far, they appear to have developed as identifiable pearlite lamellae in a much shorter growth distance. Fig. 13 illustrates eutectoid decomposition in the Ti–Ni alloy in a situation where the broad faces of parallel proeutectoid α plates were somewhat further apart. Note that at these interphase boundaries the individual Ti_2Ni crystals appear to have developed quite differently, being both shorter and fatter and appearing, *ab initio*, as palpably isolated crystals nucleated at well-defined partially coherent α : β boundaries. In the area of Fig. 13, the bainite reaction clearly prevailed. This pair of micrographs strongly suggests that pearlitic and bainitic eutectoid structures can become such during a quite early stage in their development, rather than gradually evolving into one or the other of these eutectoid decomposition mechanisms.

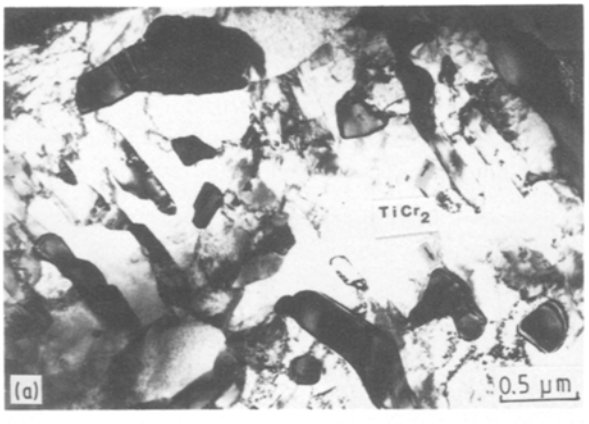

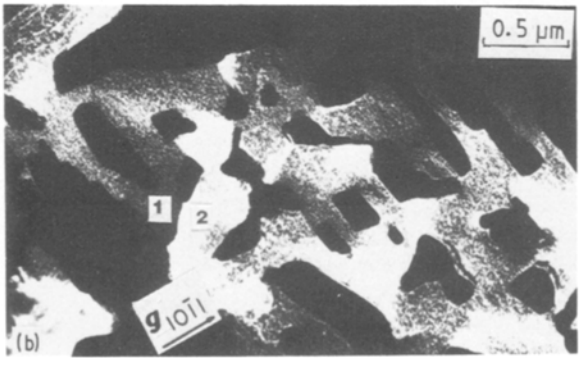

4. Discussion

4.1. Proeutectoid alpha reaction

In respect of the TEM results reported on this transformation, only two comments are necessary. The first is that the important role which the hithero largely neglected phenomenon of sympathetic nucleation plays in the lengthening of proeutectoid α plates has been further emphasized in this study. Particularly in view of a recent theoretical demonstration that development of morphological complexity by branching is almost always crystallographically impossible for the common orientation relationships amongst fcc, bcc and hcp crystals [8] (and is thus unlikely to be feasible when more complex crystal structures are involved) sympathetic nucleation appears likely now to be recognized as an important factor in a number of other transformations. For example, the intricate branching mechanism which has been presented for the development of additional cementite lamellae during the pearlite reaction in steel [3] may well be extensively dependent upon sympathetic nucleation rather than continuous growth for the frequent and often drastic changes in boundary orientation which this mechanism requires.

The results reported also emphasize the ubiquity of partially coherent interphase boundary structures. Even quite intricately shaped proeutectoid α crystal(s) (especially in Fig. 4) turned out to be partially coherent at all observable orientations. Additionally, the difficulty of relating the growth ledge structure of a precipitate crystal to its shape has become

Figure 9 Bright-field micrograph of bainite microstructure in Ti–7.15 wt % Cr alloy reacted at 893 K for 8.65×10^{-5} sec, showing elongated eutectoid $TiCr_2$ crystals. (b) Dark-field micrograph of the same area taken from $(1\,0\,1\,1)_\alpha$ reflection, illustrating contrast between adjacent areas of eutectoid α, e.g. 1 and 2. (c) Higher magnification bright-field micrograph of part of the same area, illustrating small-angle boundaries between eutectoid α crystals.

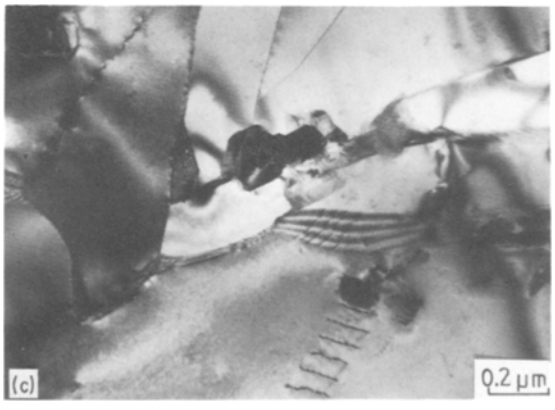

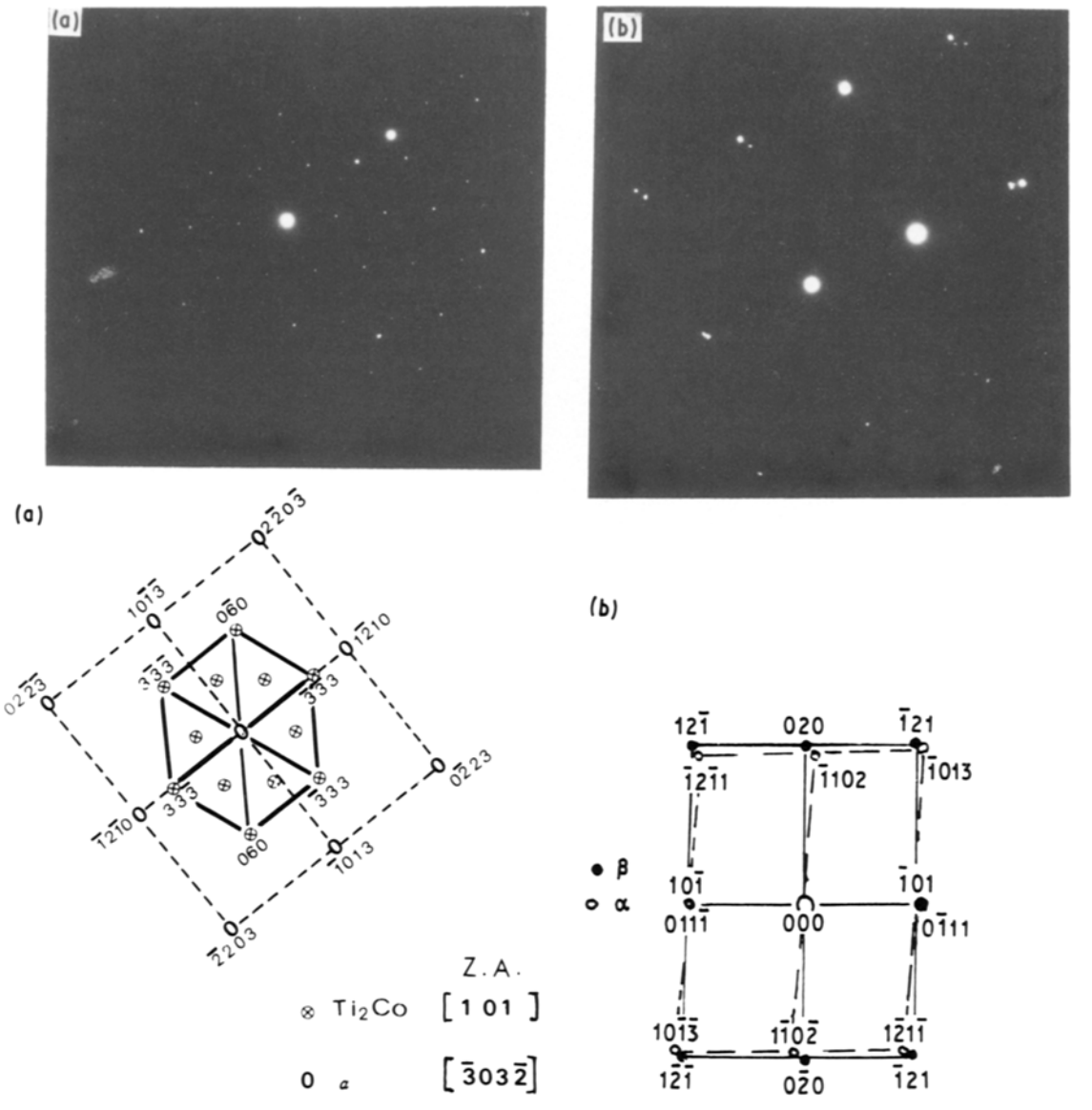

Figure 10 SAD and indexed patterns illustrating orientation relationships in Ti–3.9 wt % Co reacted at 898 K for 7200 sec; (a) between Ti_2Co and α, showing $(0\,0\,0\,1)_\alpha \parallel (0\,1\,1)_{Ti_2Co}$, $[1\,\bar{2}\,1\,0]_\alpha \parallel [1\,1\,\bar{1}]_{Ti_2Co}$ orientation relationship; (b) between α and β phases, showing Burger's orientation relationship.

particularly apparent. The intertwined systems of growth ledges observed thus would not have been anticipated on the basis of external α morphology alone. However, it is necessary to consider the growth ledge structure actually present in order to account realistically for experimentally observed growth kinetics.

4.2. Bainite reaction

4.2.1. Orientation relationships

The finding that rational orientation relationships obtain amongst α, β and intermetallic compound crys-

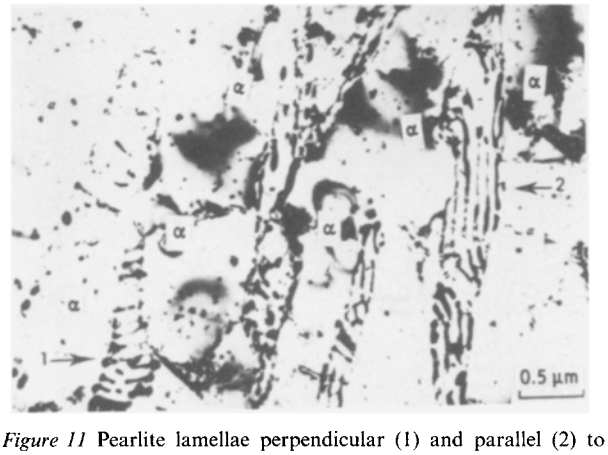

Figure 11 Pearlite lamellae perpendicular (1) and parallel (2) to proeutectoid α plates in Ti–4.0 wt % Ni reacted at 1003 K for 1200 sec.

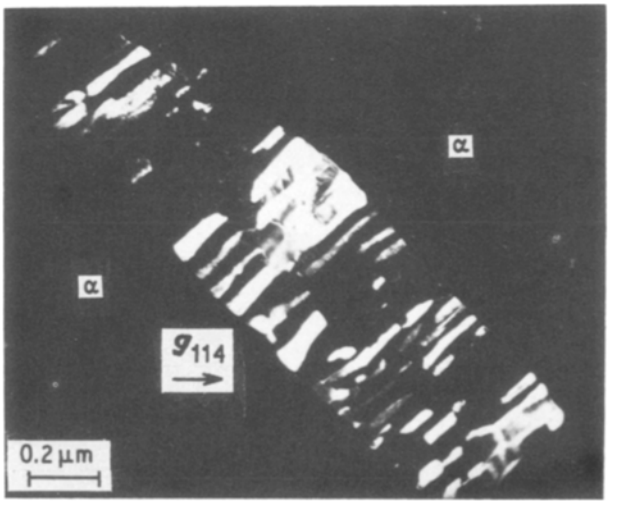

Figure 12 Pearlite lamellae growing directly from broad faces of closely spaced parallel proeutectoid α plates in Ti–6.0 wt % Cu reacted for 60 sec at 998 K.

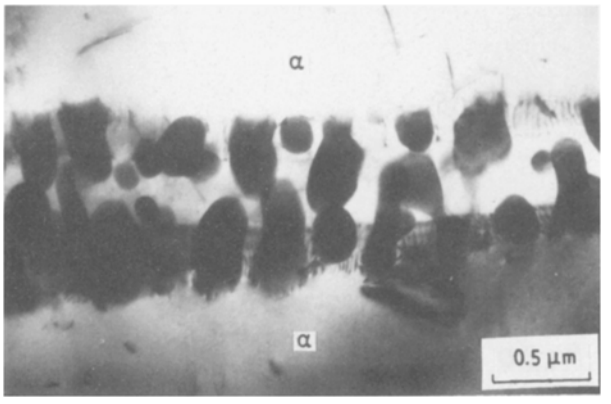

Figure 13 Bainite formed at broad faces of closely spaced, parallel proeutectoid α plates in Ti–4.0 wt % Ni reacted at 1003 K for 1200 sec.

tals in bainite in at least three Ti–X systems (Table III), is equivalent to counterpart observations made on $M_{23}C_6$ carbides precipitated in association with grain-boundary ferrite allotriomorphs formed in Fe–C–Cr alloys [35]. While the orientation relationships determined during the present investigation developed during compound precipitation at α sideplates and/or intragranular plates, it has long been apparent that the differences between grain-boundary allotriomorphs and the various Widmanstatten morphologies of a given precipitate phase are not fundamental [14, 36]. Earlier, it was considered that the ratio of disordered boundary area to partially coherent boundary area is appreciably higher at allotriomorphs than at the Widmanstatten morphologies [14, 36]. It is now becoming apparent, however, that the areas of allotriomorph: matrix boundaries which appear curved at low magnifications (and are thus, presumably, disordered) may actually be made up of many, closely spaced ledges [34], and thus also are largely partially coherent. Carbides have been shown to precipitate at the broad faces or terraces of ledges, rather than at the risers of ledges on austenite : ferrite boundaries [27, 28, 37]. Although the interfacial energy of risers is higher than that of terraces, the highly mobile risers will overrun and destroy embryos before they reach critical nucleus size, whereas the lower energy terraces, being immobile, will not [38]. Attempts to demonstrate that carbides precipitate at disordered austenite : ferrite boundaries [39] have been experimentally disproved [40]. Present indications are that a grain-boundary allotriomorph usually has a "standard", low indices-type orientation relationship with respect to one matrix grain and a higher indices relationship (but one which is still capable of producing partially coherent boundaries) with respect to the adjacent matrix grain [41, 42]. When carbides form at the high index orientation relationship boundary of an allotriomorph, a different, "non-standard" set of orientation relationships is to be expected between the carbides and the ferrite and the austenite lattices. However, when the carbides form at that broad face of an allotriomorph which has the "standard" low indices orientation relationship with respect to its austenite grain, the same types of orientation relationships amongst the three phases as are found when the carbides nucleate at proeutectoid ferrite sideplates and intragranular plates, appear likely. These considerations are consistent with both the absence of unusual orientation relationships found during the present investigation, wherein the "carbides" or intermetallic compound crystals were nucleated only at α plate morphologies, and with their presence during some studies of carbide precipitation at grain-boundary allotriomorphs in Fe–C–X alloys [28, 39]. Clearly, though, extension of such studies to both allotriomorphs and plates in a given alloy now appears to be necessary.

4.2.2. Morphology of bainite

In both the Ti–Co (Figs 5a and b) and Ti–Cu (Fig. 6) alloys studied, the bainitic intermetallic compound crystals formed at the proeutectoid α plates are small and approximately equiaxed. In the Ti–Cr alloy (Fig. 9), on the other hand, these crystals are decidedly elongated in the overall growth direction of the bainitic α + compound structure. Differences of this type are considered theoretically in another paper in this series [31]. When growth of the two product phases of a eutectoid reaction by the ledge mechanism was introduced into a linearized concentration gradient analysis [43] of the edgwise growth of pearlite, it was found that these two phases can grow side by side at the same rate only when the ratio of the height (h) to the average inter-ledge spacing (λ) on the interphase boundaries of both is the same. (This statement is based upon the assumption that the equilibrium proportions of the two product phases are formed; in the non-equilibrium situation, a slightly more complicated relationship must be fulfilled.) In the case of bainite, these ratios differ. The phase with the higher ratio grows more rapidly and thus tends to overgrow the other phase and terminate its access to the matrix. This process, however, will normally lead to the renucleation of the slower growing phase at the interphase boundaries of the faster growing phase. In a hypereutectoid Ti–25 wt % Cr alloy, where the eutectoid $TiCr_2$ crystals also tend to be elongated in the growth direction of the bainite structure, the non-equilibrium version of the h/λ ratio for eutectoid $TiCr_2$ was found to be indistinguishable from that for eutectoid α within the quite wide limits of experimental error [31]. The theoretical analysis would predict that in the Ti–Co and Ti–Cu bainites examined during the present investigation the appropriate form of the h/λ relationship would be significantly less for the compound than for α. Unfortunately, the kinetics with which eutectoid α surrounds eutectoid compound crystals in these alloys proved to be too rapid to permit the TEM observations required to test this prediction to be made.

In the Ti–X alloy systems studied by Franti *et al.* [1] and the present investigators, as well as in the Ti–Cr alloys investigated earlier [5, 43], bainite microstructures in hypoeutectoid alloys are fully equivalent to upper bainite in hypoeutectoid steels, i.e. plates of proeutectoid α with isolated intermetallic compound crystals precipitated at the boundaries between them. In the parallel theoretical study, however, the conclusion was reached that the intrinsic external

morphology of bainite is the nodule, approximately spherical in shape when nucleated intragranularly and hemispherical when developed at grain-boundary allotriomorphs [4]. The familiar plate morphology of bainite evolves when the two-phase microstructure of eutectoid α + eutectoid intermetallic compound develops epitaxially on proeutectoid α plates and thereby replicates their morphology. Similarly, the interphase-boundary precipitation of intermetallic compound initiated at grain-boundary allotriomorphs, followed by eutectoid α formation which more or less symmetrically enlarges the allotriomorphs [27, 28], is the morphology which bainite develops when grain-boundary allotriomorphs are a prominent feature of the microstructure, as in certain high-alloy hypoeutectoid Fe–C–X alloys in which X inhibits sideplate formation [6, 44]. The nodule morphology has the opportunity to develop only when the volume fraction of proeutectoid phase is small and/or relatively large, roughly equiaxed volumes of matrix phase are available into which the bainite structures can grow. Additionally, eutectoid α must be able to grow into the matrix phase *away* from the proeutectoid α crystals at which it first appeared. This could occur as a combined result of the boundary orientation-dependence of interphase-boundary structure, growth mechanism and kinetics and of the accelerated motion of those area of eutectoid $\alpha:\gamma$ boundaries where β crystals have nucleated close together [4, 44]. To date, bainite nodules have been observed in hypoeutectoid titanium-base alloys only in a high-oxygen (0.30 wt %) Ti–10.94 wt % Cr alloy [5]. Perhaps because the high concentration of chromium restricted the proportion of proeutectoid α which could form and/or because oxygen accelerated coarsening of the proeutectoid α microstructure, sufficiently bulky volumes of untransformed β were available in the vicinity of grain-boundary α allotriomorphs to give the nodule structure the "space" in which to develop. It is not anticipated that nodular structures will be often found in hypoeutectoid Ti–X alloys, however, because of the potent tendency of Widmanstatten α plates to form voluminously and in close proximity to each other when undercooling below the $\beta/(\alpha + \beta)$ transus temperature is sufficient so that the reaction temperature is below that of eutectoid [43].

4.2.3. Origins of pearlite and bainite

The presently accepted view of pearlite formation [3] is based on the assumption that the edges of the lamellae of both participating phases are disordered. Pearlite is taken to evolve gradually as these phases "learn" to grow together, "cooperatively", in side-by-side fashion, to their mutual kinetic advantage. Pearlite formation was suggested to be favoured by predominantly disordered interphase boundaries round crystals of the proeutectoid phase, and bainite formation was taken to prosper in the presence of partially coherent boundaries on this phase [3]. This non-crystallographic view of pearlite formation has now been seriously compromised by the finding of some evidence for misfit dislocations at the edge of pearlite lamellae in an Fe–C–Mn alloy [45], and especially by the observation that these lamellae lengthen by means of shared growth ledges [46]. Also as previously noted, the broad faces of grain-boundary allotriomorphs in the Ti–7.15 wt % Cr alloy are extensively ledged; λ/h often lies in the range 2 to 4 [34] rather than the order-of-magnitude higher values usually encountered at the broad faces of plates [14, 20]. Fig. 12 of this paper makes a further contribution toward a crystallographic view of pearlite formation by providing evidence that "cooperative" growth develops at a very early stage of transformation.

On the non-crystallographic view of pearlite evolution [3], a disordered interphase boundary on a proeutectoid crystal is a preferred site at which to initiate this process, because the disordered boundary structure, taken to be independent of boundary orientation, provides the flexibility needed to develop cooperative growth. Conversely, a partially coherent boundary lacks this flexibility and hence the non-cooperative eutectoid decomposition product known as bainite develops instead. However, this viewpoint is inconsistent with the new experimental evidence on the interphase boundary structure of grain-boundary allotriomorphs just cited. Thus it is now suggested that pearlite as well as bainite develops from partially coherent boundaries on crystals of the proeutectoid phase. However, those interphase boundaries at which h/λ is very small will encourage the bainitic mechanism of eutectoid decomposition because the relatively long distance between adjacent risers seriously limits the flexibility of the boundary needed to evolve cooperative growth. The present investigation has shown that fresh nucleation of proeutectoid α (now termed eutectoid α), either sympathetically or at compound : matrix boundaries, is often required to displace the $\alpha:\beta$ boundaries enclosing sideplates and intragranular plates. Simple continuation of growth, as postulated by Hultgren [30], is evidently inhibited, at least in hypoeutectoid Ti–X alloys, unless more growth ledges develop at the $\alpha:\beta$ interface in association with compound formation at this interface.

On the other hand, pearlite formation should be facilitated at the interphase boundaries of those proeutectoid phase crystals at which h/λ is comparatively large. As a consequence of the high density of growth ledges, such boundaries should now have the potential to develop appreciable "manoeuverability", particularly if: (i) not too many ledges are stepped consecutively in the same direction, and (ii) diffusional interactions between adjacent ledges [47, 48] cause merging of small ledges into larger ones, thereby accomplishing large changes in local boundary orientation. Enomoto [49] has recently shown that when growth ledges are closely spaced the overall growth kinetics approach those of a disordered interphase boundary. This result provides a good explanation for the reasonable agreement usually obtained between the experimentally measured growth kinetics of grain-boundary ferrite allotriomorphs in Fe–C alloys and those calculated assuming that the allotriomorphs are oblate ellipsoids of revolution with disordered austenite : ferrite boundaries [50]. Somewhat more speculatively, the authors offer the suggestion

that the limitations upon manoeuverability of interphase boundaries which remain even when growth ledges are closely spaced may be further mitigated through the formation of pearlitic ferrite by sympathetic nucleation. Although Hillert [3] has brilliantly demonstrated with the multiple sectioning technique that the lamellae in a pearlite colony in steel derive from repeated branching of a single crystal of ferrite and a single crystal of cementite, the optical microscopy observational technique employed may have been unable to detect the 1 to 2° or smaller misorientations which appear to accompany sympathetic nucleation [8].

5. Conclusions

Franti *et al.* [1] have reported an optical microscopy study of the microstructurally defined [2–4] bainite reaction in ten Ti–X eutectoid systems. In the present investigation, these studies have been pursued further on representative hypoeutectoid alloys by means of transmission electron microscopy in five Ti–X systems, where X was successively cobalt, chromium, copper, iron and nickel. Related studies have also been conducted on the proeutectoid α and the pearlite reactions in these alloys.

Supplementing a recent detailed investigation performed on a hypoeutectoid Ti–Cr alloy [8], edge-to-edge sympathetic nucleation of proeutectoid α plates has been identified in a Ti–3.9 wt % Co alloy. Small-angle boundaries again separate the freshly nucleated α crystal from the one against which it formed. For the first time, the ledge structure has been followed continuously around the leading edge of an α lath on to the side edges of the lath. Whereas the ledges are both closely and regularly spaced at the leading edge, they are quite far apart and irregularly spaced at the side edges. These observations are consistent with the high and uniform lengthening kinetics of plates and needles which have been accepted for decades [15] and with the slower kinetics which necessarily characterize the sidewise growth of a lath. Multiple ledge systems have been identified on proeutectoid α plates or laths whose presence is not advertised by the shape of these crystals but which must be taken into account when evaluating their growth kinetics.

The following orientation relationships were determined amongst the three phases participating in the formation of bainite:

$$\text{Ti–4.0 wt \% Ni: } (0\,1\,1)_\beta \parallel (0\,0\,0\,1)_\alpha \parallel (0\,1\,1)_{Ti_2Ni}$$

$$[1\,1\,1]_\beta \parallel [1\bar{2}\,1\,0]_\alpha \parallel [1\,1\,\bar{1}]_{Ti_2Ni}$$

$$\text{Ti–3.9 wt \% Co: } (0\,1\,1)_\beta \parallel (0\,0\,0\,1)_\alpha \parallel (0\,1\,1)_{Ti_2Co}$$

$$[1\,1\,\bar{1}]_\beta \parallel [1\,1\,\bar{2}\,0]_\alpha \parallel [1\,1\,\bar{1}]_{Ti_2Co}$$

$$\text{Ti–7.15 wt \% Cr: } (0\,1\,1)_\beta \parallel (0\,0\,0\,1)_\alpha \parallel (0\,1\,1)_{TiCr_2}$$

$$[1\,1\,\bar{1}]_\beta \parallel [1\,1\,1\,\bar{2}\,0]_\alpha \parallel [2\,1\,\bar{1}]_{TiCr_2}$$

The Burgers orientation relationship is seen always to obtain between α and β. The intermetallic compounds Ti_2Ni and Ti_2Co have the same spatial orientation as β; these compounds have the same complex f c c ($E9_3$) crystal structure; the same parallel planes but different parallel directions obtained between β and $TiCr_2$, an f c c-type C15 compound. In the case of α–compound relationships, $(0\,0\,0\,1)_\alpha \parallel (0\,1\,1)_{cpd}$ in all three systems, but again Ti_2Ni and Ti_2Co have the same direction parallel to its counterpart in α while $TiCr_2$ has a different direction parallel to an α direction of the same form. The presence of rational orientation relationships amongst the three phases involved is equivalent to the crystallographic situation sometimes obtaining amongst austenite, ferrite and $M_{23}C_6$ during bainite formation in association with grain-boundary allotriomorphs in an Fe–C–Cr alloy [35].

Eutectoid α was observed to be slightly misoriented with respect to immediately adjacent proeutectoid α. This suggests that eutectoid α formation in Ti–X bainite may occur by sympathetic nucleation at proeutectoid $\alpha:\beta$ boundaries rather than by continued growth of the proeutectoid α crystals, as is the Hultgren [30] mechanism, though eutectoid α nucleation at β: compound boundaries cannot be wholly excluded.

Whereas compound crystals in bainite structures formed in Ti–Co and Ti–Cu alloys are roughly equiaxed, those in Ti–Cr are pronouncedly elongated in the growth direction of the bainite structure. On a theoretical treatment of the differences between pearlite and bainite formation [31], these morphological differences suggest that the value of the ratio of the growth ledge height to the average spacing between growth ledges, h/λ, for intermetallic compound crystals is much smaller than that for eutectoid α in Ti–Co and Ti–Cu, but approaches that for eutectoid α in Ti–Cr.

In respect of the pearlite reaction, only in Ti–Cu is this a major mode of eutectoid decomposition in hypoeutectoid alloys amongst the Ti–X eutectoid systems investigated to date [1, 51]. The present study has disclosed the presence of pearlite in a Ti–4.0 wt % Ni alloy between proeutectoid α sideplates so closely spaced that the pearlite structure could not have been resolved during the previous optical microscopy study [1]. The lamellae in some of the pearlite colonies in this alloy were orthogonal to the broad faces of the side plates and must thus have developed from partially coherent $\alpha:\beta$ boundaries, in contradiction to the presently accepted mechanism for pearlite evolution [3]. Recent experimental observations provide preliminary evidence for closely spaced ledges on grain-boundary α allotriomorphs in a Ti–Cr alloy [34]. This observation seems likely to be general. Allotriomorphs have long been recognized as an excellent site for the development of pearlite [3, 52]. Hence it appears that pearlite as well as bainite may develop from partially coherent interphase boundaries on crystals of the proeutectoid phase. The suggestion was accordingly offered that bainitic eutectoid structures develop when h/λ at these boundaries is small and that pearlitic structures can evolve when h/λ is relatively large. In the bainite situation, when $h/\lambda \ll 1$, the average boundary orientation is rather inflexible. This is consistent with the nucleation of isolated intermetallic compound crystals at $\alpha:\beta$ boundaries which are subsequently surrounded by eutectoid α. In the

case of pearlite, where $h/\lambda < 1$, there is appreciable flexibility in the average orientation of the $\alpha:\beta$ boundaries. Hence some "cooperation" between α and compound growth, which is the central feature of the Hillert [3] mechanism for pearlite formation, can develop. However, the limitations upon flexibility placed by the immobility of the terraces between ledges [14, 36] suggests that sympathetic nucleation of pearlitic α may be needed (as appears to occur in bainite) to complete the cooperation process.

Acknowledgement

Appreciation is expressed to the US Air Force Office of Scientific Research for support of this research through Grant AFOSR84-0303.

References

1. G. W. FRANTI, J. C. WILLIAMS and H. I. AARONSON, *Met. Trans.* **9A** (1978) 1641.
2. H. I. AARONSON, "The Mechanism of Phase Transformations in Crystalline Solids" (Institute of Metals, London, 1969) p. 270.
3. M. HILLERT, "Decomposition of Austenite by Diffusional Processes", edited by V. F. Zackay and H. I. Aaronson (Interscience, New York, 1962) p. 197.
4. H. J. LEE and H. I. AARONSON, *Acta Metall.* in press.
5. H. I. AARONSON, W. B. TRIPLETT and G. M. ANDES, *Trans. TMS-AIME* **209** (1957) 1227.
6. *Idem, ibid.* **212** (1958) 624.
7. H. J. LEE, G. SPANOS, G. J. SHIFLET and H. I. AARONSON, *Acta Metall.* in press.
8. E. S. K. MENON and H. I. AARONSON, *ibid.* **34** (1986) 1963.
9. *Idem, ibid.* **34** (1986) 1975.
10. *Idem, ibid.* **35** (1987) 549.
11. D. BANERJEE and J. C. WILLIAMS, *Scripta Metall.* **17** (1983) 1125.
12. G. G. WEATHERLY and T. D. MOK, *Surface Sci.* **31** (1972) 355.
13. H. GLEITER, *Acta Metall.* **17** (1969) 565.
14. H. I. AARONSON, C. LAIRD and K. R. KINSMAN, "Phase Transformations", edited by H. I. Aaronson (ASM, Metals Park, Ohio, 1970) p. 313.
15. E. P. SIMONEN and R. TRIVEDI, Report to U.S.A.E.C., Iowa State University, Ames, Iowa (August, 1972).
16. H. I. AARONSON and C. LAIRD, *Trans. TMS-AIME* **242** (1968) 1437.
17. C. LAIRD and H. I. AARONSON, *Acta Metall.* **17** (1969) 505.
18. E. P. SIMONEN, H. I. AARONSON and R. TRIVEDI, *Met. Trans.* **4** (1973) 1239.
19. J. W. CAHN, W. B. HILLIG and G. W. SEARS, *Acta Metall.* **12** (1964) 1421.
20. H. I. AARONSON, *J. Microscopy* **102** (1974) 275.
21. C. LAIRD and H. I. AARONSON, *Trans. TMS-AIME* **242** (1968) 242.
22. *Idem, Acta Metall.* **15** (1967) 73.
23. K. CHATTOPADHYAY and H. I. AARONSON, *ibid.* **34** (1986) 713.
24. D. J. H. COCKAYNE, *J. Microscopy* **98** (1973) 116.
25. J. K. LEE and H. I. AARONSON, *Acta Metall.* **23** (1975) 799.
26. *Idem, ibid.* **23** (1975) 809.
27. R. W. K. HONEYCOMBE, *Met. Trans.* **7A** (1976) 915.
28. *Idem, Met. Sci. J.* **14** (1980) 201.
29. P. D. FROST, W. M. PARRIS, L. L. HIRSCH, J. R. DOIG and C. M. SCHWARTZ, *Trans. ASM* **46** (1954) 231.
30. A. HULTGREN, *ibid.* **39** (1947) 915.
31. H. J. LEE and H. I. AARONSON, *Acta Metall.* in press.
32. M. HANSSEN, "Constitution of Binary Alloys", 2nd Edn (McGraw-Hill, New York, 1958) pp. 511, 1049.
33. M. HILLERT, personal communication, Carnegie–Mellon University (1985).
34. T. FURUHARA, A. M. DALLEY and H. I. AARONSON, unpublished research, Carnegie–Mellon University, (1986).
35. P. R. HOWELL, J. V. BEE and R. W. K. HONEYCOMBE, *Met. Trans.* **10A** (1979) 1213.
36. H. I. AARONSON, "Decomposition of Austenite by Diffusional Processes", edited by V. F. Zackay and H. I. Aaronson (Interscience, New York, 1962) p. 387.
37. A. T. DAVENPORT and R. W. K. HONEYCOMBE, *Proc. Roy. Soc.* **322** (1971) 191.
38. H. I. AARONSON, J. K. LEE and K. C. RUSSELL, "Precipitation Processes in Solids" (TMS-AIME, Warrendale, Pennsylvania, 1978) p. 31.
39. R. A. RICKS and P. R. HOWELL, *Acta Metall.* **31** (1983) 853.
40. T. OBARA, G. J. SHIFLET and H. I. AARONSON, *Met. Trans.* **14A** (1983) 1159.
41. M. R. PLICHTA and H. I. AARONSON, *Acta Metall.* **28** (1980) 1041.
42. J. K. PARK and A. J. ARDELL, *ibid.* **34** (1986) 2399.
43. M. HILLERT, *Met. Trans.* **3** (1972) 2729.
44. P. G. BOSWELL, K. R. KINSMAN, G. J. SHIFLET and H. I. AARONSON, "Mechanical Properties and Phase Transformations in Engineering Materials – Earl R. Parker Symposium on Structure Property Relationships" (TMS-AIME, Warrendale, Pennsylvania, 1986) p. 467.
45. S. A. HACKNEY and G. J. SHIFLET, *Acta Metall.* **35** (1987) 1007.
46. *Idem, Scripta Metall.* **19** (1985) 757.
47. G. J. JONES and R. TRIVEDI, *J. Crystal Growth* **29** (1975) 155.
48. C. ATKINSON, *Proc. Roy. Soc. London* **A384** (1982) 197.
49. M. ENOMOTO, *Acta Metall.* **35** (1987) 935, 947.
50. J. R. BRADLEY, J. M. RIGSBEE and H. I. AARONSON, *Met. Trans.* **8A** (1977) 323.
51. J. C. WILLIAMS, D. H. POLONIS and R. TAGGART, "The Science, Technology and Application of Titanium", edited by R. I. Jaffee and N. E. Promisel (Pergamon, London, 1970) p. 733.
52. H. I. AARONSON, *Trans. TMS-AIME* **212** (1958) 212.

Received 11 February
and accepted 29 April 1987